

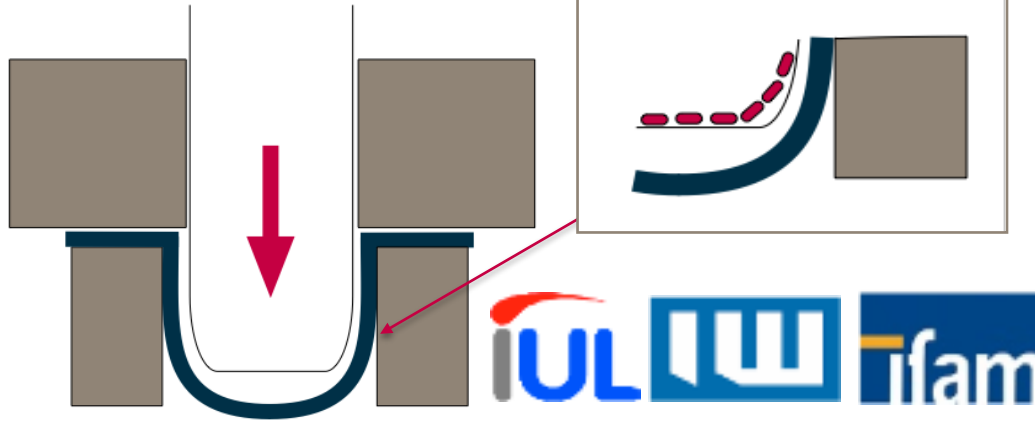
# Parameter identification for combined quasi-static / electromagnetic forming processes by mathematical optimization

Marco Rozgic, Marcus Stiemer

I<sup>2</sup>FG Meeting, Nantes, 2016



# Combining fast and quasi-static forming methods



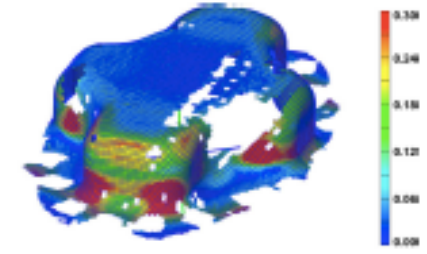
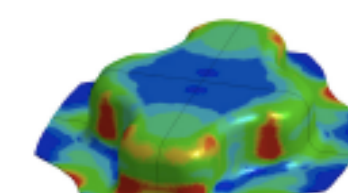
**iuliu ifam**



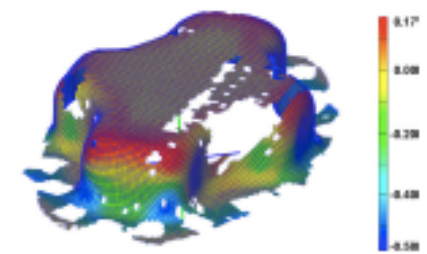
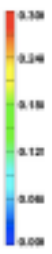
(a) Simulation: Major strain



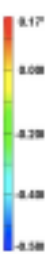
(c) Simulation: Minor strain



(b) Experiment: Major strain



(d) Experiment: Minor strain

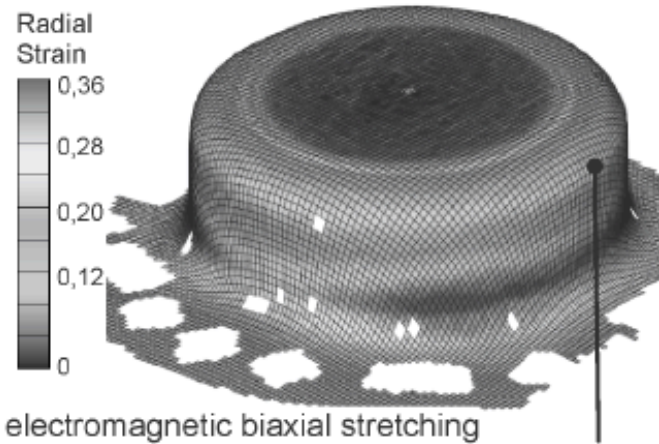
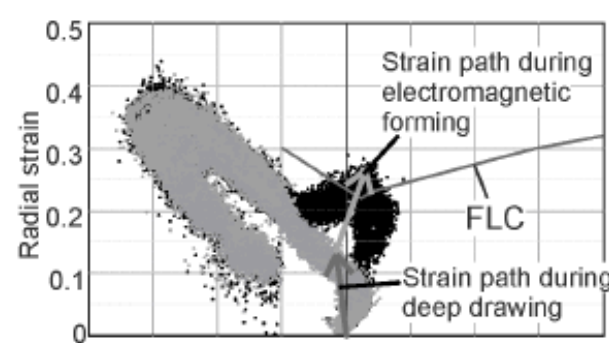


## Motivation

- Combination of two methods may increase the freedom of design
- Integration in existing tools is possible
- Profit from advantages of a contact-free method
- Design of tailored processes for complicate forming tasks
- Combination of fast and quasi-static methods yields forming beyond quasi static forming limits

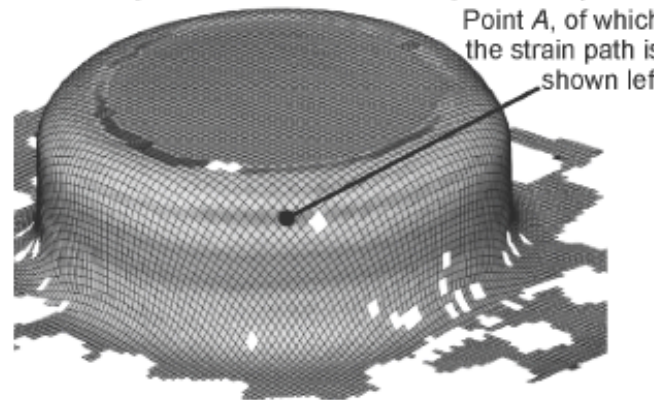
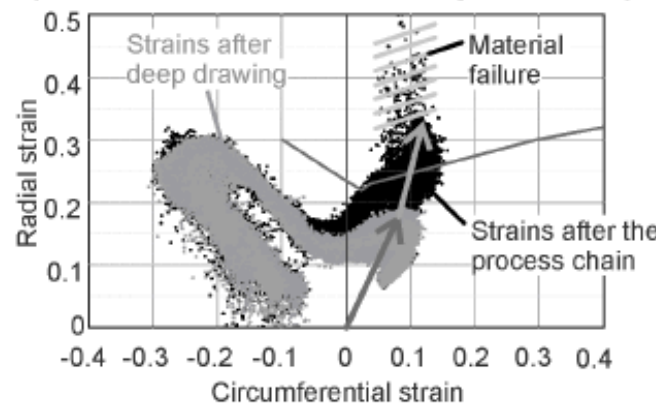
# Enhanced formability due to combination with impulse methods

a) Quasi-static plane strain stretching followed by electromagnetic biaxial stretching



Material: EN A-5083

b) Quasi-static biaxial stretching followed by electromagnetic biaxial stretching



Experimental results



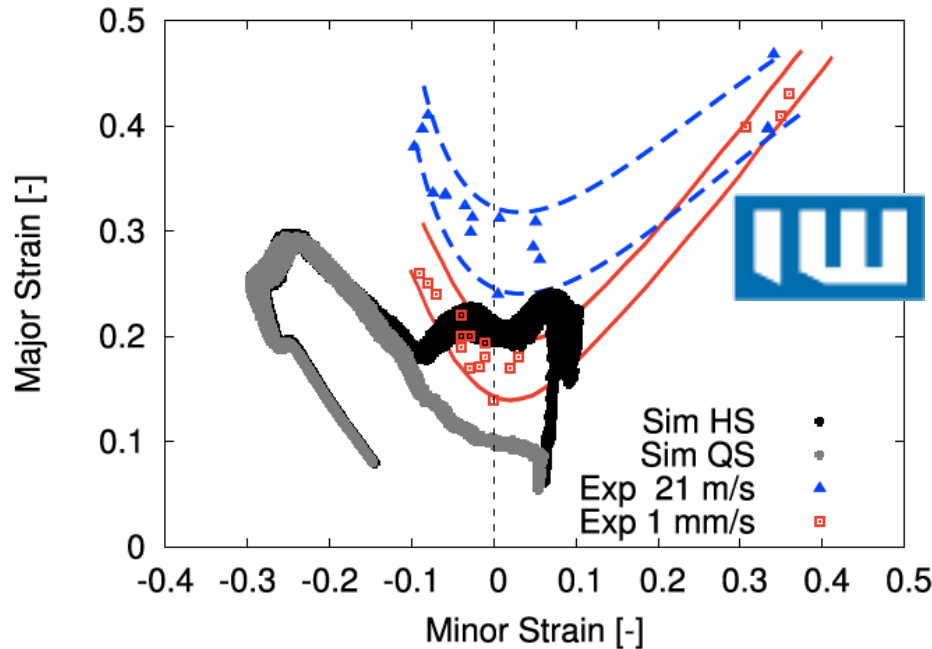
Kiliclar, Y., Demir, O.K., Engelhardt, M., Rozgic, M., Vladimirov, I.N., Wulfinghoff, S., Weddeling, C., Gies, S., Klose, C., Reese, S., Tekkaya, A.E., Maier, H.J., Stiemer, M., 2016:

*Experimental and numerical investigation of increased formability in combined quasi-static and high-speed forming processes.*

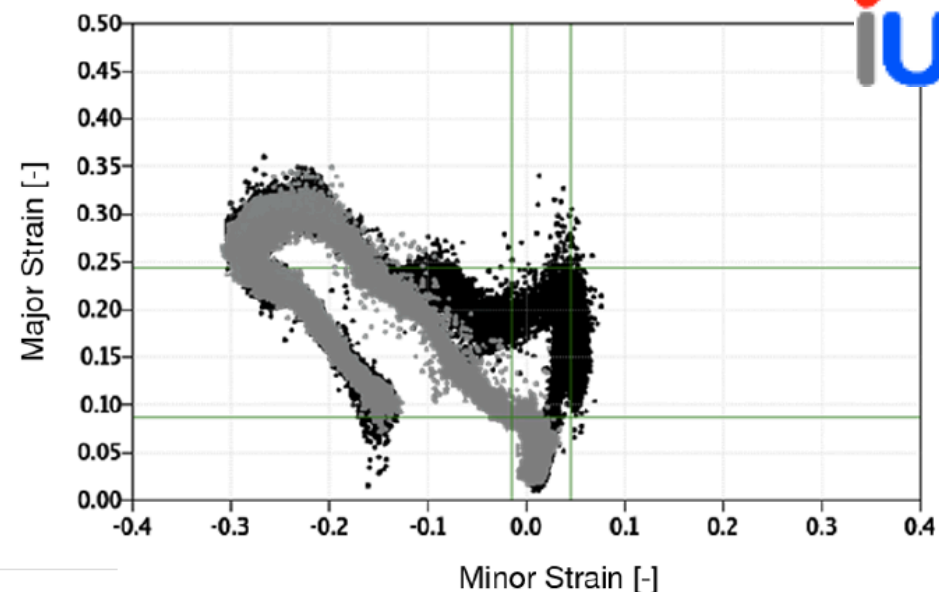
Journal of Materials Processing Technology, Volume 237, S. 254-269.

# On the quality of simulation results and the usability of FLCs

Simulated with LS-DYNA



(a) Simulation



(b) Experiment

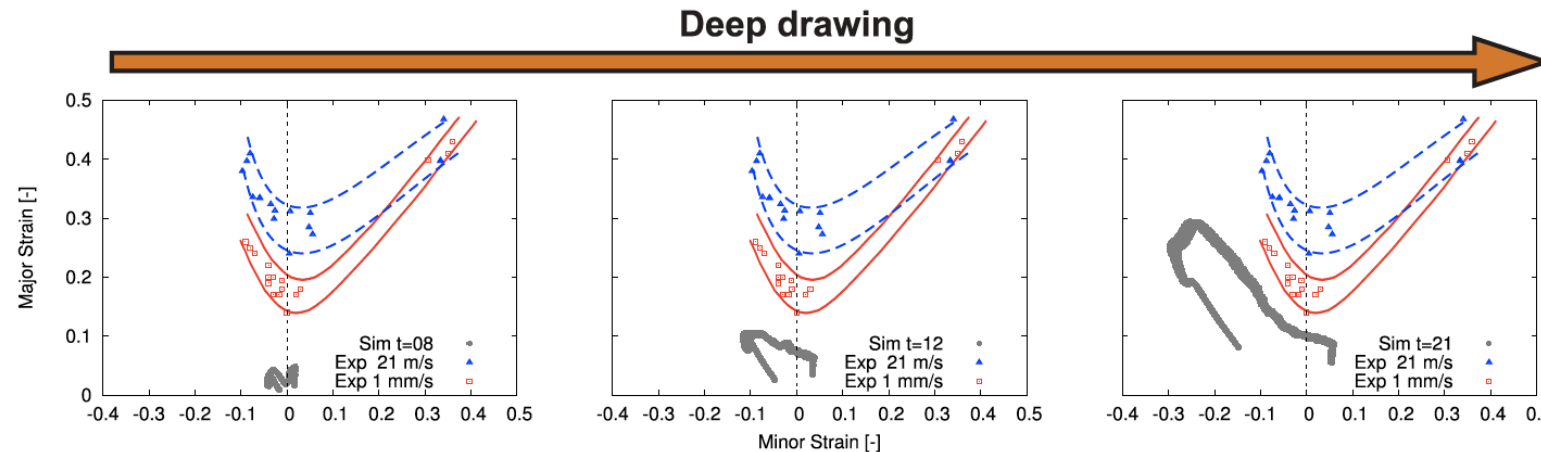
Corresponding strain rates: 1000 1/s 0.1 1/s

Kiliclar, Y., Demir, O.K., Engelhardt, M., Rozgic, M., Vladimirov, I.N., Wulfinghoff, S., Weddeling, C., Gies, S., Klose, C., Reese, S., Tekkaya, A.E., Maier, H.J., Stiemer, M., 2016:

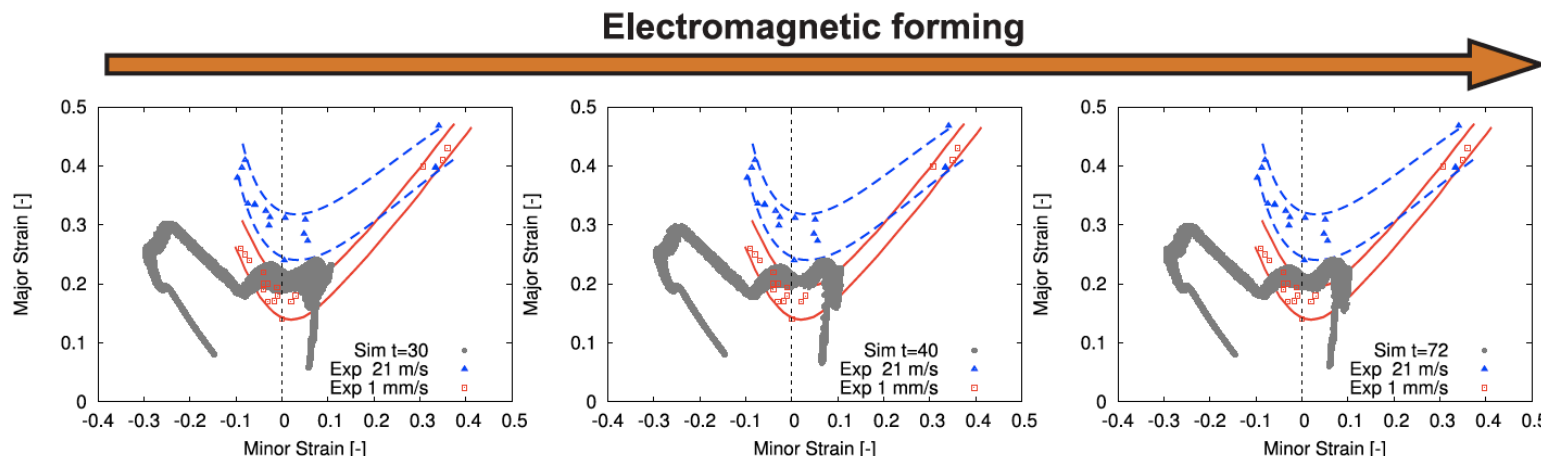
*Experimental and numerical investigation of increased formability in combined quasi-static and high-speed forming processes.*

Journal of Materials Processing Technology, Volume 237, S. 254-269.

# Evolution of strains



(a) Initial deep drawing step



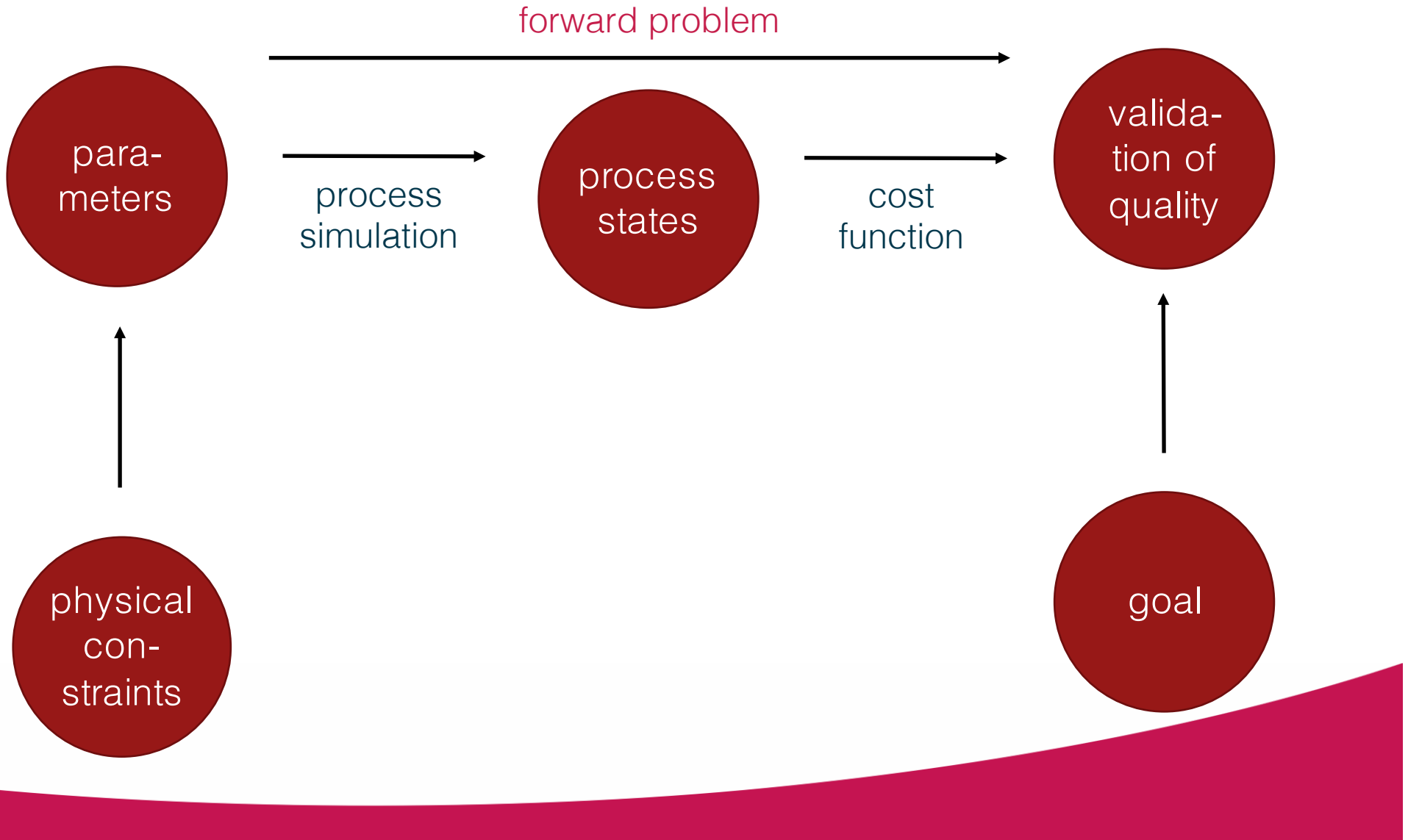
(b) Subsequent high-speed forming step

FLCs by  
**EW**

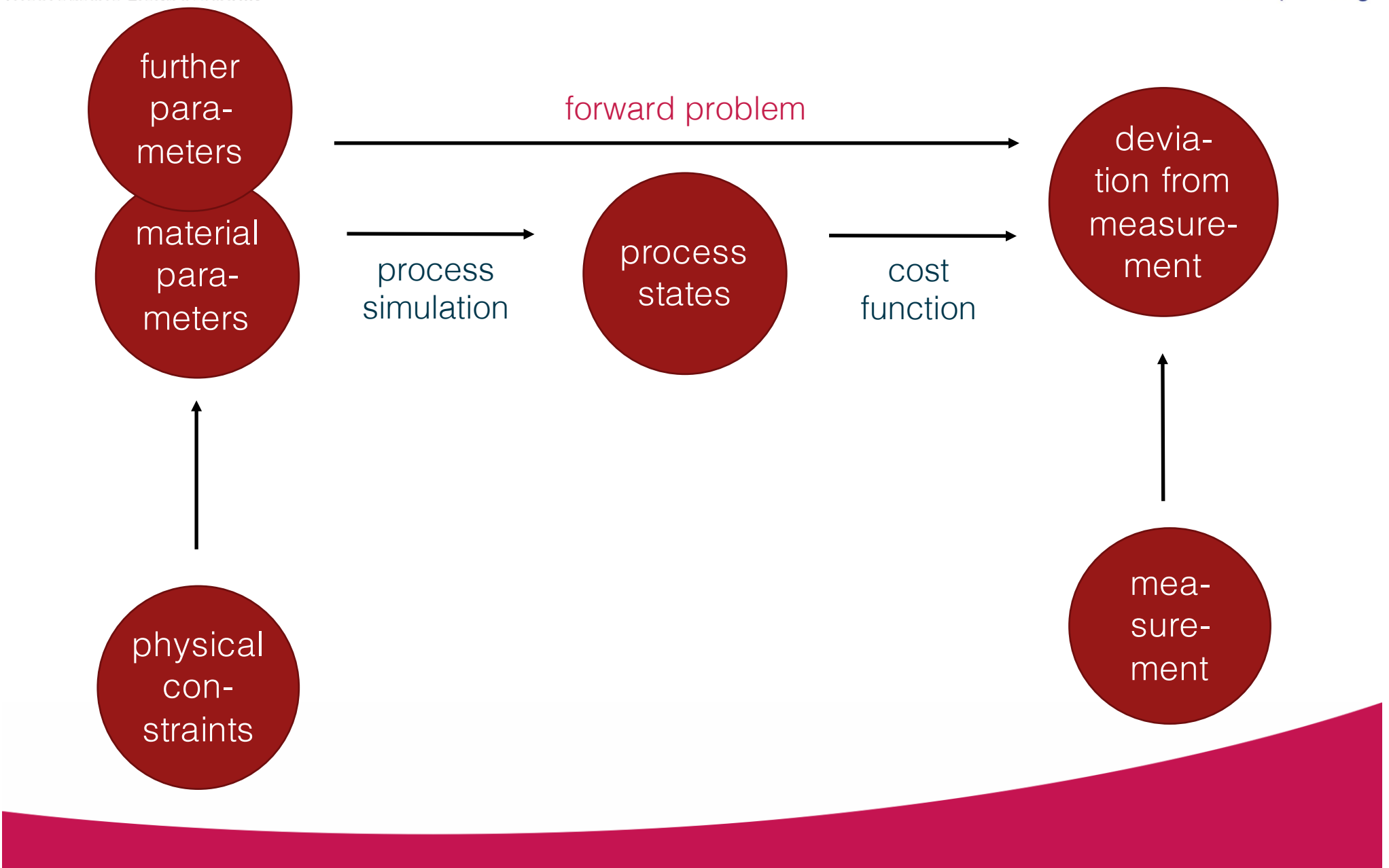
## Need for mathematical optimization

- Mathematical Optimization can generally be used to solve identification problems, e.g., to identify
- process parameters that lead to a process with favorable properties (e.g., an extension of forming limits)
- internal parameters of the employed material model

# Mathematical optimization for general identification problems



# Mathematical optimization for material parameters



Stress-strain  
Relation

Hill-type yield function

Plastic multiplier (Perzyna  
formulation)

Isotropic hardening

Kinematic hardening

Damage (Lemaitre)

# One model for all stages

$$S = \mu (C_p^{-1} - C^{-1}) + \frac{\lambda}{2} \left( \det C (\det C_p)^{-1} - 1 \right) C^{-1}, \quad X = c (C_{p_i}^{-1} - C_p^{-1})$$

$$Y = CS - C_p X, \quad Y_{\text{kin}} = C_p X$$

$C$  Cauchy-Green tensor

$$\Phi = \sqrt{Y^D \cdot (\tilde{\mathcal{A}} [(Y^D)^T])} - \sqrt{\frac{2}{3}} (\sigma_y + Q (1 - e^{-\beta \kappa}))$$

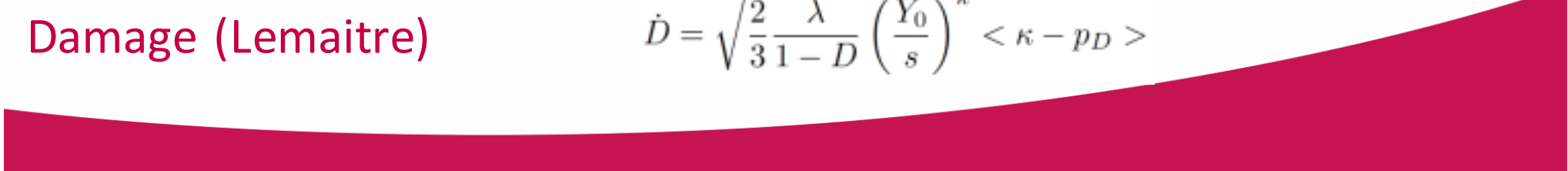
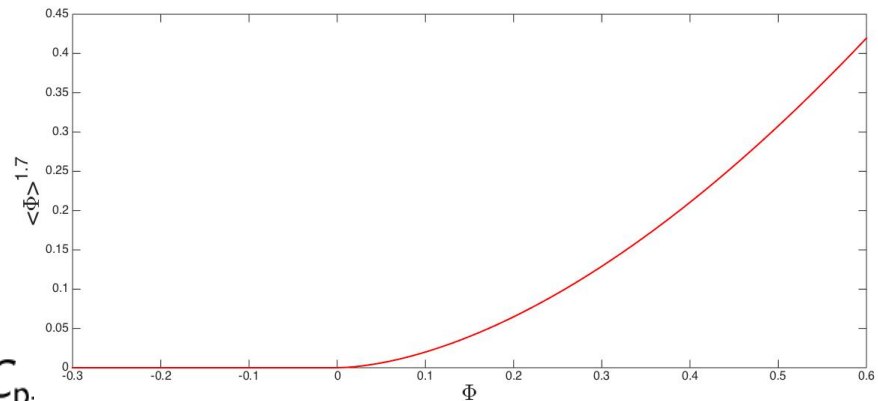
With a stress like tensor  $Y$  derived from the second Piola-Kirchoff tensor  $S$  and backstress  $X$

$$\dot{\Lambda} = \frac{\langle \Phi \rangle^m}{\eta}$$

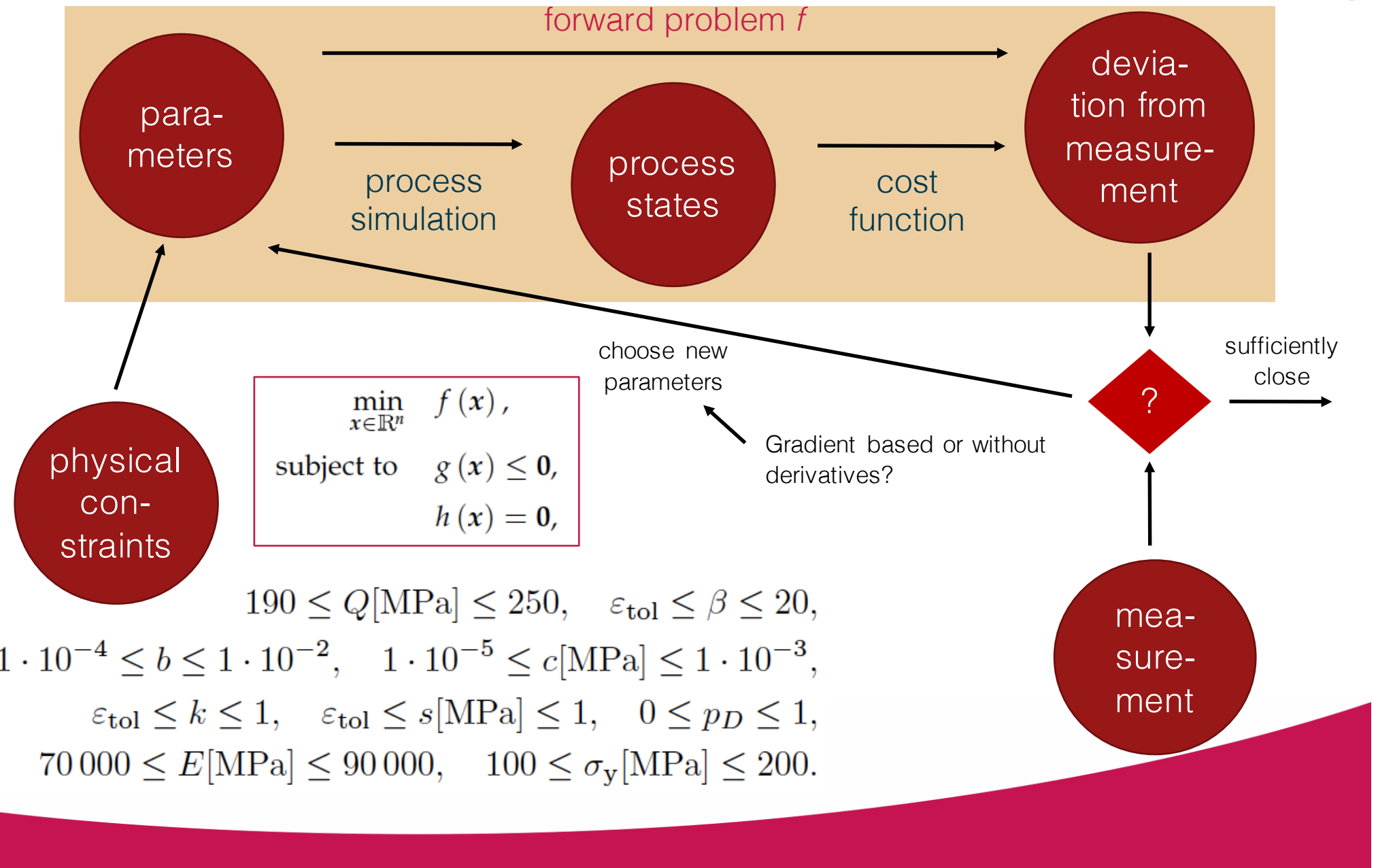
$$\dot{\kappa} = \sqrt{\frac{2}{3}} \dot{\Lambda}$$

$$\dot{C}_{p_i} = 2 \dot{\Lambda} \frac{b}{c} Y_{\text{kin}}^D C_{p_i}$$

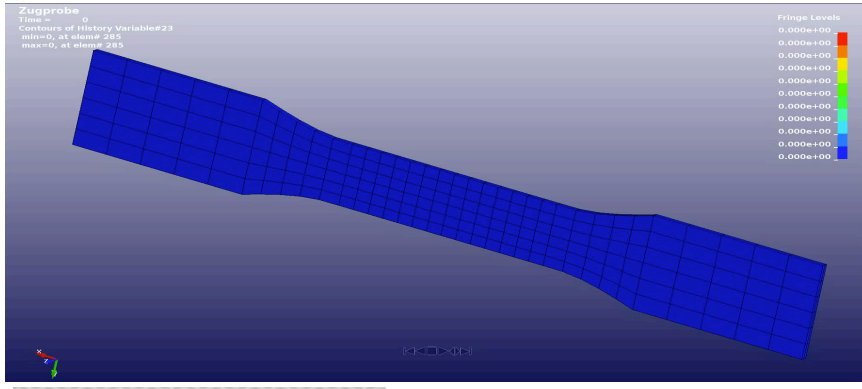
$$\dot{D} = \sqrt{\frac{2}{3}} \frac{\dot{\lambda}}{1 - D} \left( \frac{Y_0}{s} \right)^k < \kappa - p_D >$$



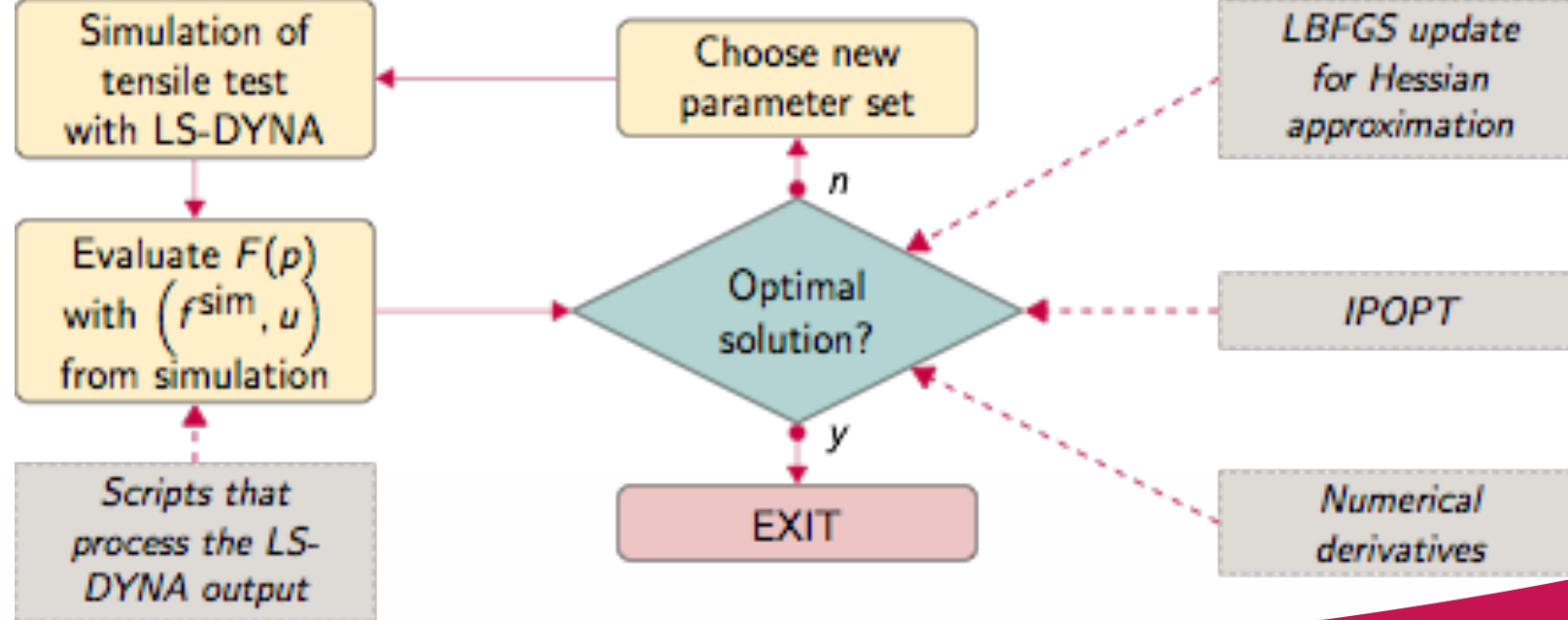
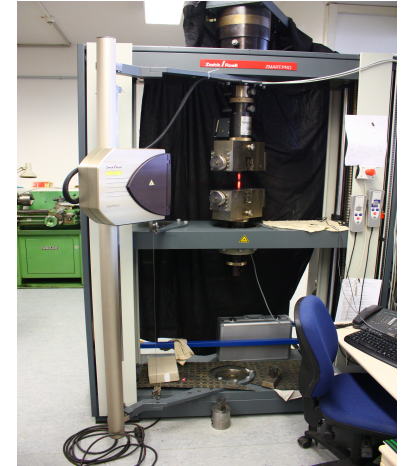
# The inverse problem



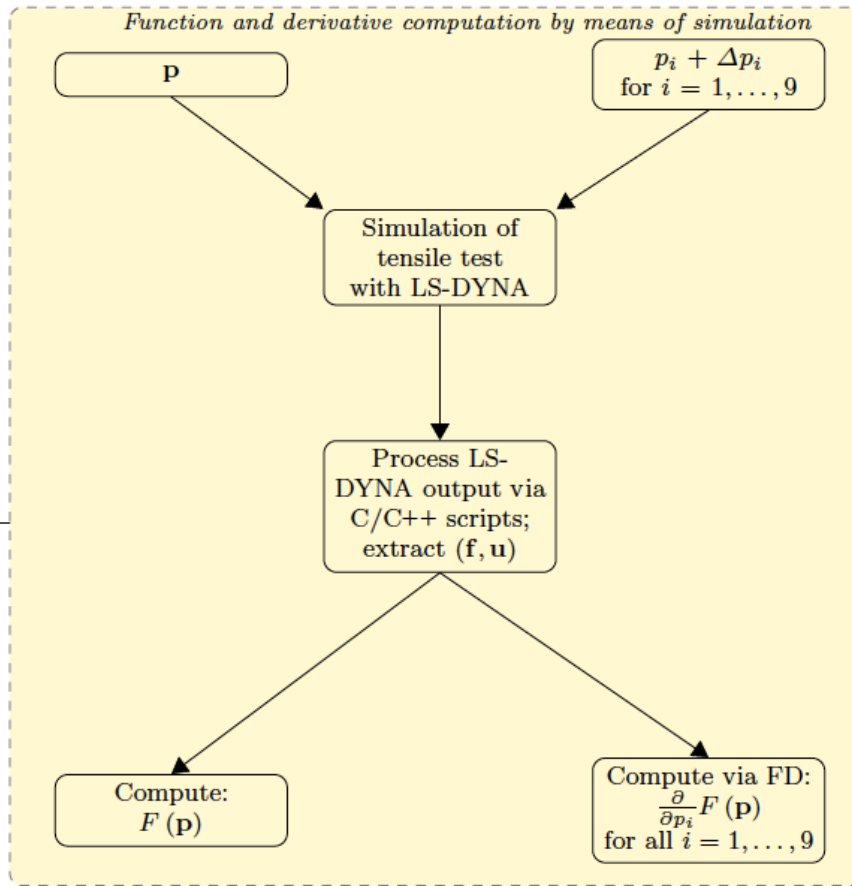
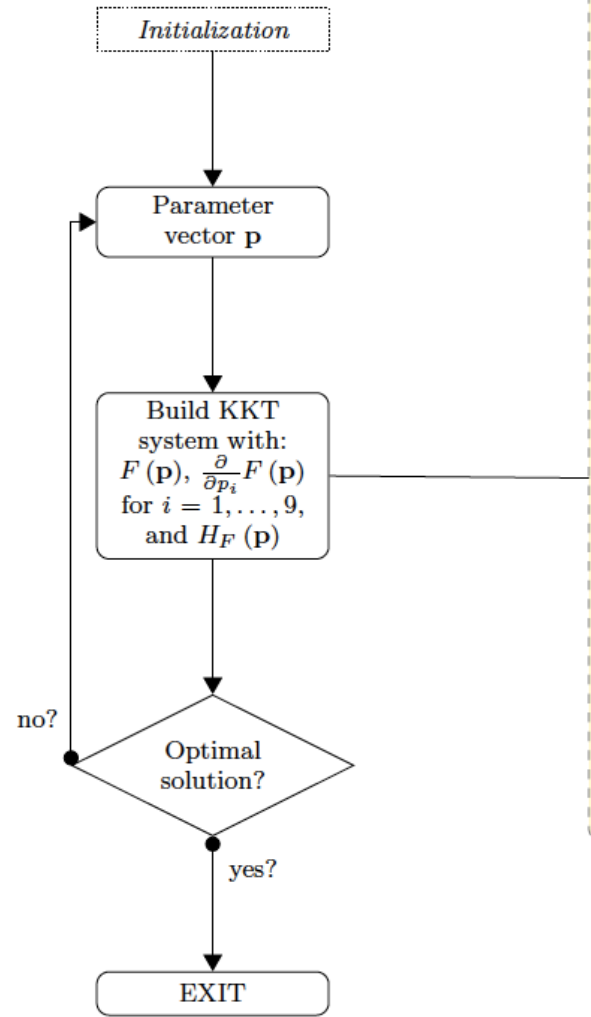
# Identification of the material model



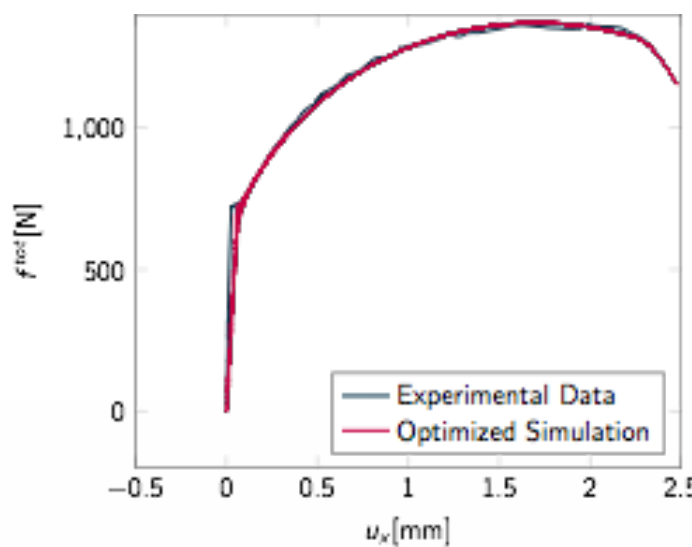
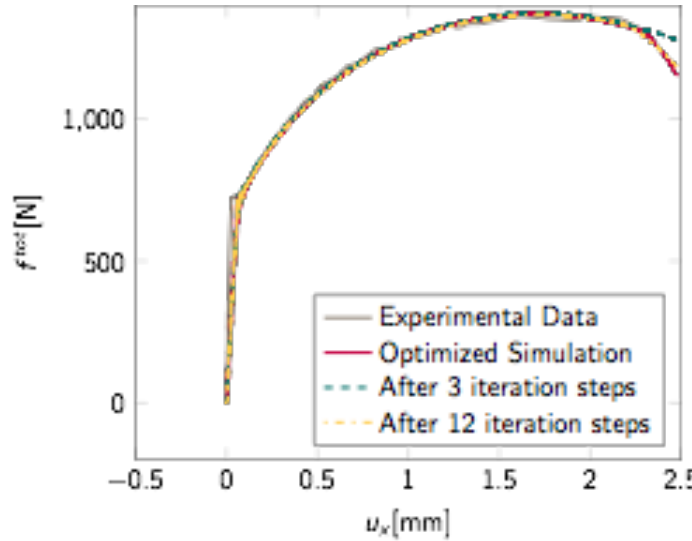
*Initial parameter set*



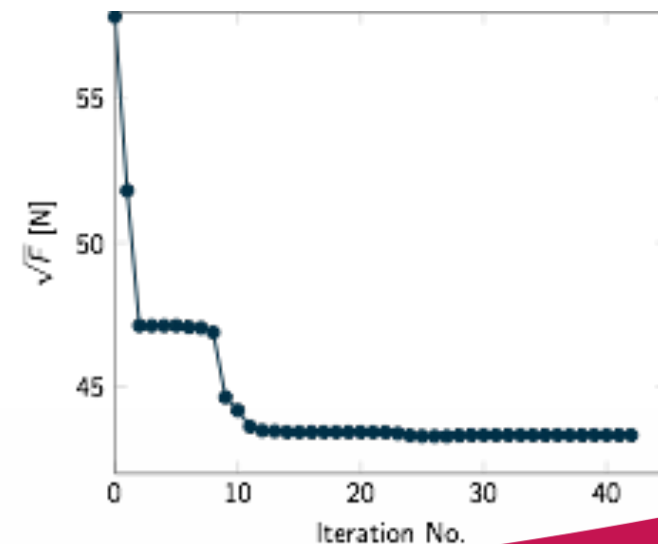
# The algorithm with numerical computation of derivatives



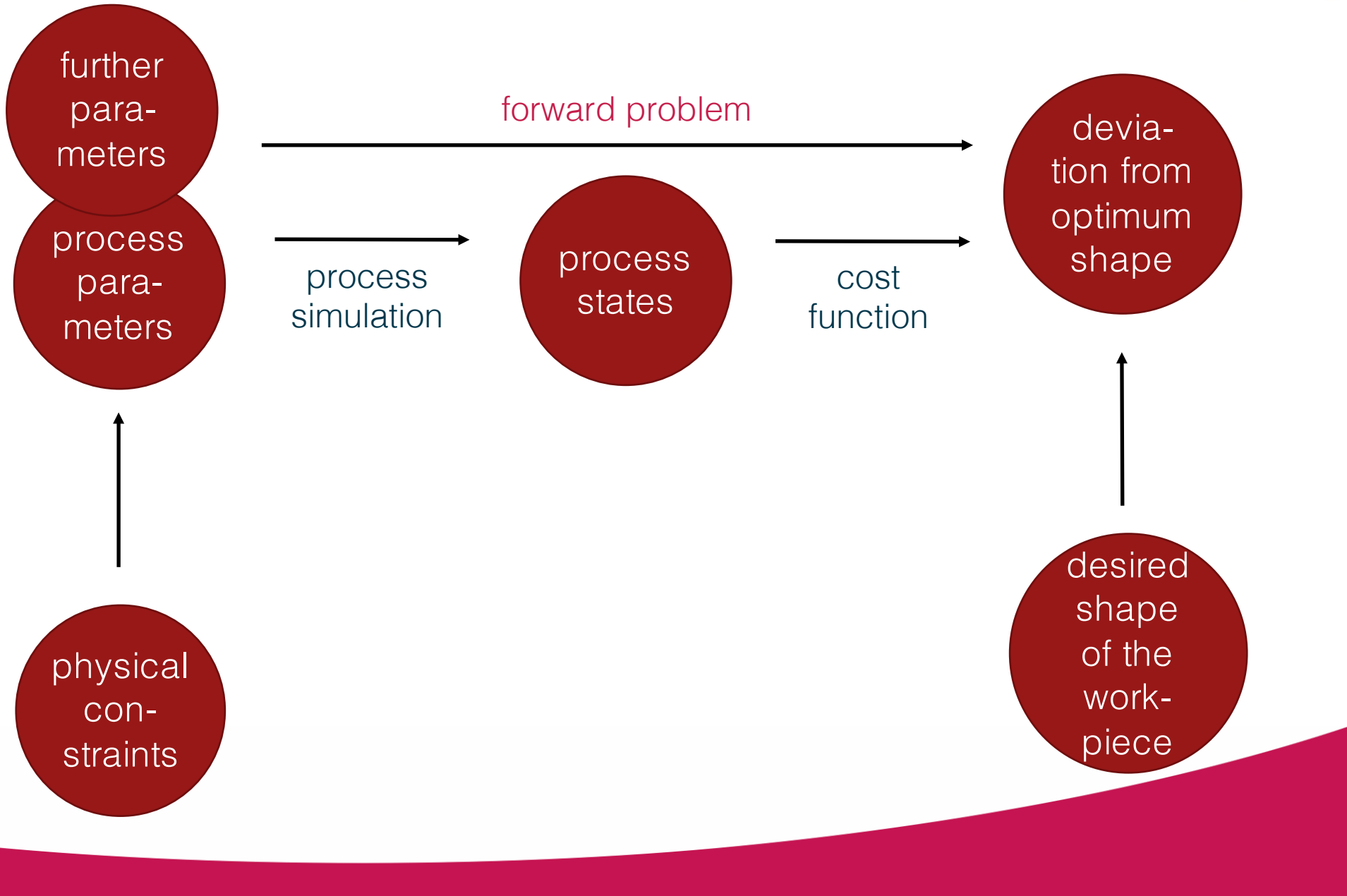
# Model identification



Young's modulus	$E$	$8,089 \times 10^4$ MPa
Yield stress (von Mises)	$\sigma_y$	$1,185 \times 10^2$ MPa
Backstress (isotropic)	$Q$	$1,604 \times 10^2$ MPa
Hardening parameter (isotropic)	$\beta$	$1,265 \times 10^1$
Hardening parameter (kinematic)	$b$	$5,124 \times 10^{-3}$
Equivalent stress (kinematic hardening)	$c$	$4,598 \times 10^{-4}$ MPa
Strain-rate-exponent	$k$	$4,694 \times 10^{-1}$
Equivalent strain for damage model	$s$	$2,680 \times 10^{-1}$
Threshold for damage	$p_D$	$6,306 \times 10^{-1}$

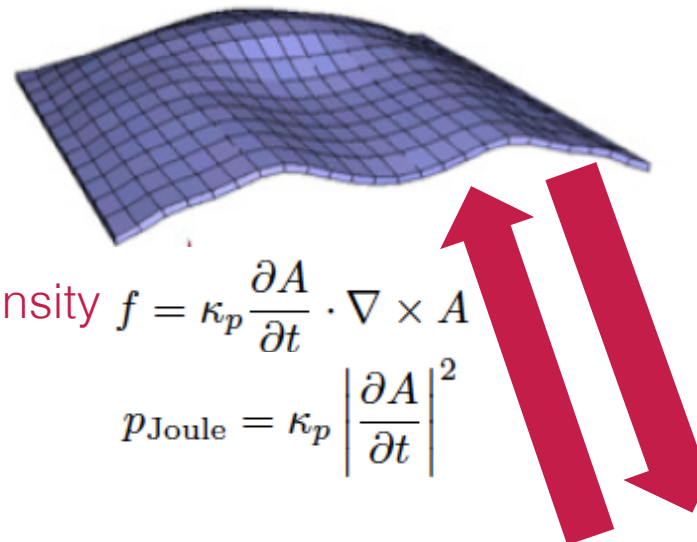


# Mathematical optimization for process parameters



# The coupled model

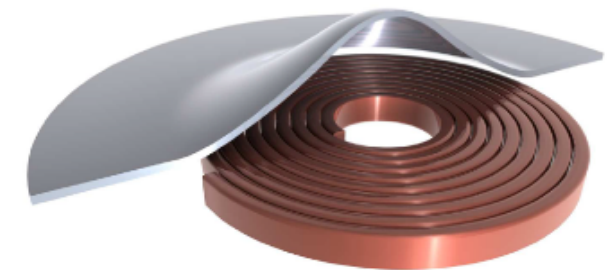
## Mechanical model



Lorentz force density  $f = \kappa_p \frac{\partial A}{\partial t} \cdot \nabla \times A$

Joule heating

$$p_{\text{Joule}} = \kappa_p \left| \frac{\partial A}{\partial t} \right|^2$$



Spatial distribution  
of conductivity  $\kappa_p$

Eddy current equation for the magnetic vector potential  $A$

$$\nabla \times \left( \frac{1}{\mu} \nabla \times \mathbf{A} \right) + \kappa_p \frac{\partial \mathbf{A}}{\partial t} = -\kappa_p \nabla \varphi_p$$



Electric scalar potential  $\Delta \varphi = 0$   
for Coloumb gauge  $\nabla \cdot A = 0$

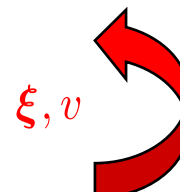
# The coupled model

Weak form of electromagnetic equations

$$\int_{\Omega} \left( \frac{1}{\mu} \nabla \times \mathbf{A} \cdot \nabla \times \tilde{\mathbf{A}} + \sigma \tilde{\mathbf{A}}^* \cdot \tilde{\mathbf{A}} \right) = - \int_S \sigma \tilde{\mathbf{A}} \cdot \nabla \phi$$

$$\int_S \nabla \phi \cdot \nabla \tilde{\phi} = 0$$

  $f_L = \det(\nabla \xi)(\mathbf{J} \times \nabla \times \mathbf{A})$   
 Lorentz-force  
 Joule heating



Weak form of mechanical force balance

$$0 = \int_{B_r} \{ \rho \ddot{\xi} - f_L \} \cdot \xi_* + \int_{B_r} K(\nabla \xi)^{-T} \cdot \nabla \xi_*$$



Material model

Unknown fields

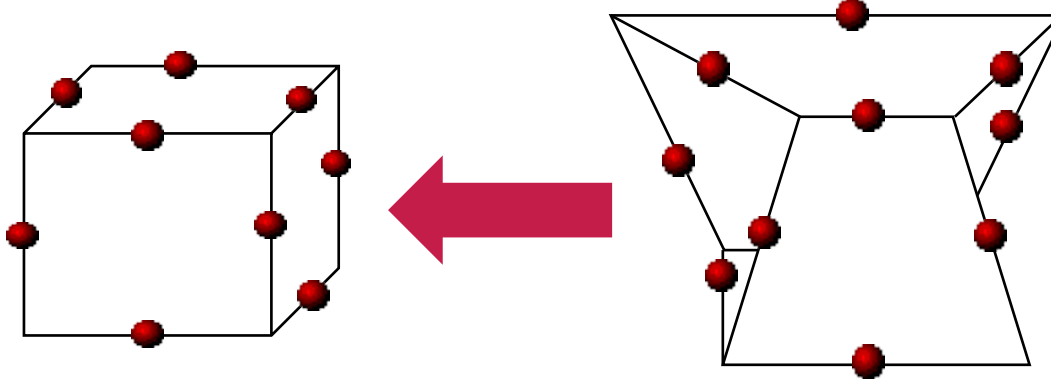
Vektorpotential  $\mathbf{A}$   
 Skalarpotential  $\Phi$   
 Deformation  $\xi$

# FE-simulation

Nédélec-elements

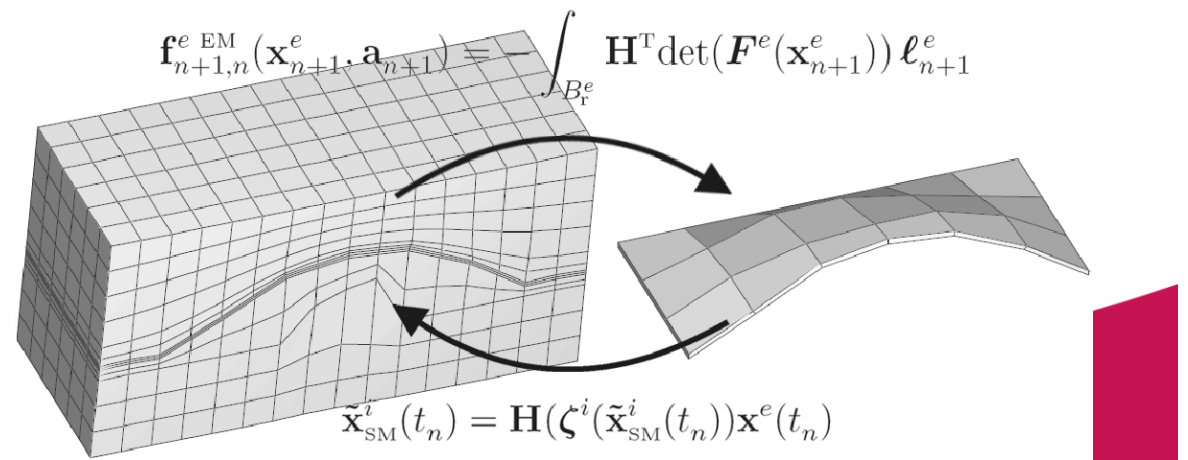
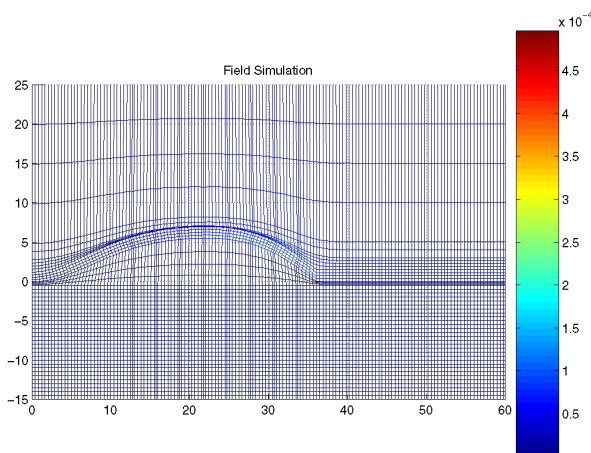
$$\int_{\Gamma_i} \mathbf{a}_e \cdot \mathbf{t}_i, \quad i = 1, \dots, 12$$

$\mathbf{t}_i$  : tangential vector



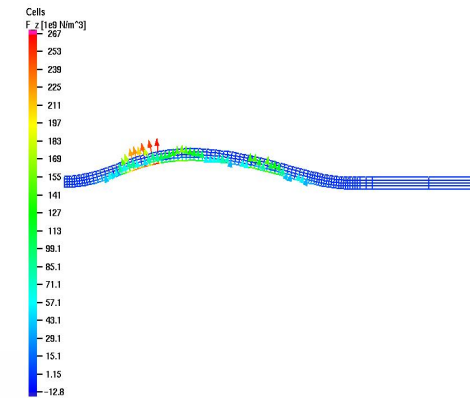
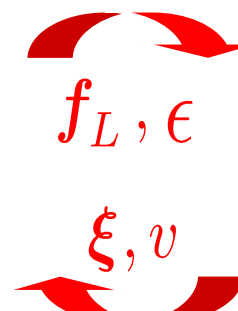
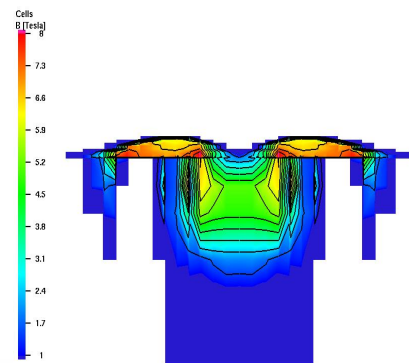
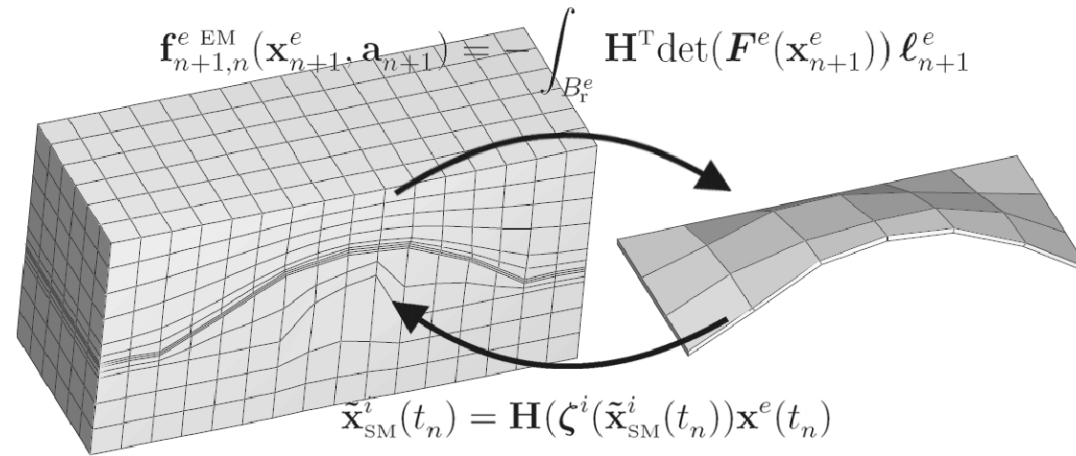
Either in the full area of interest or only in the conducting material, while boundary-elements are used in the air-gap

Arbitrary Langrangian Eulerian Formulation

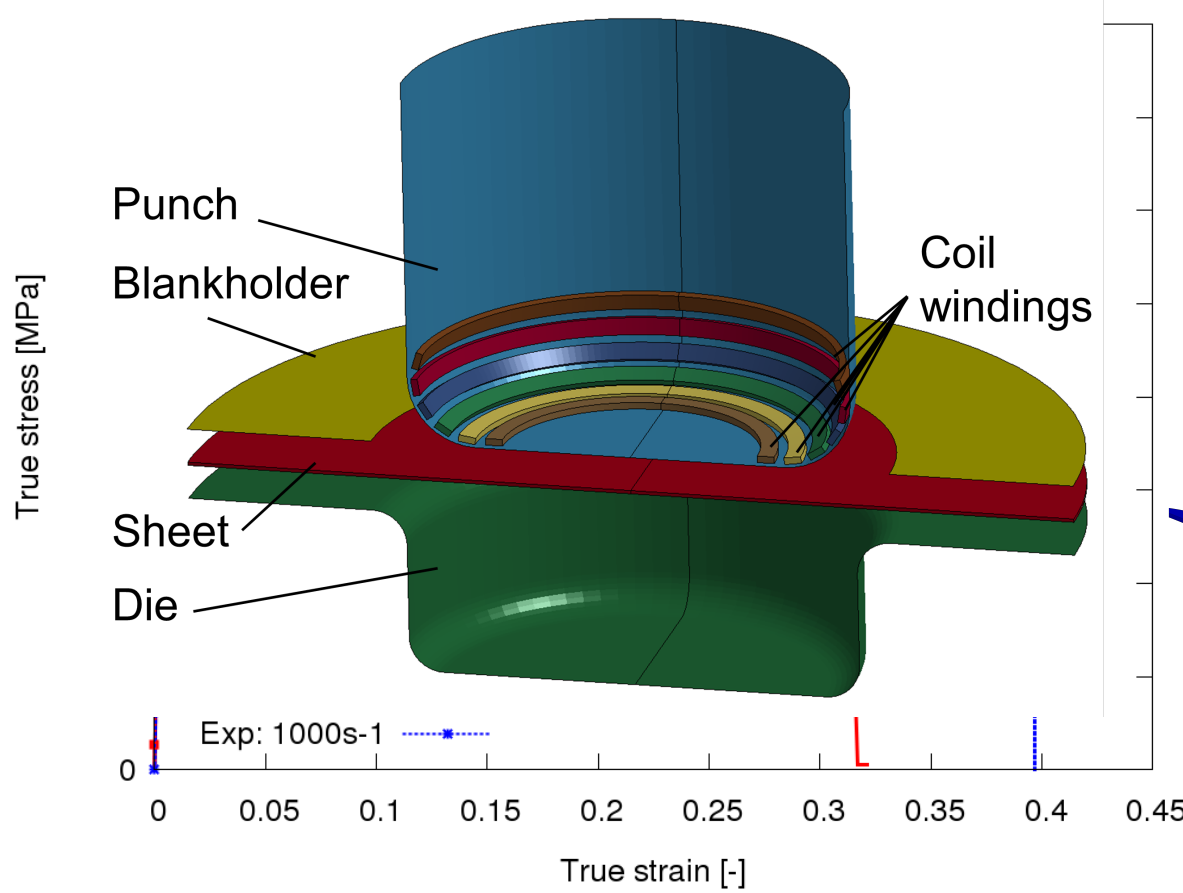


# Algorithmic coupling

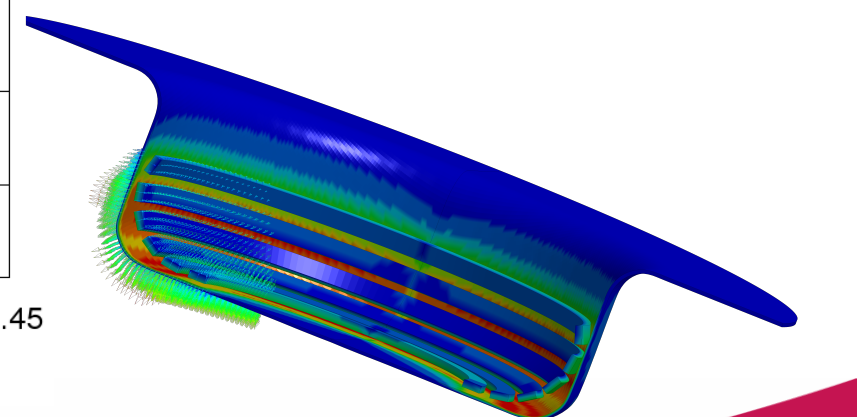
Explicit vs.  
implicit  
schemes



# Validation and verification



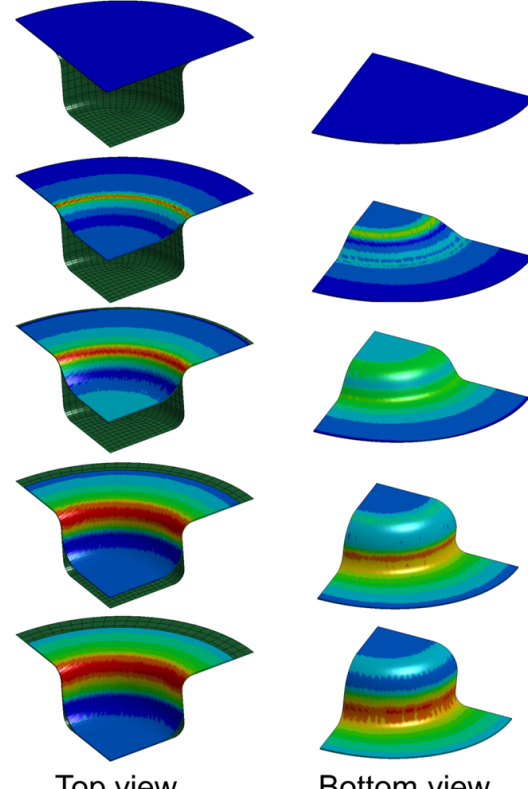
- Comparison to stress-strain curves (with evolution model for damage threshold)
- Application to complex situation (cup drawing)



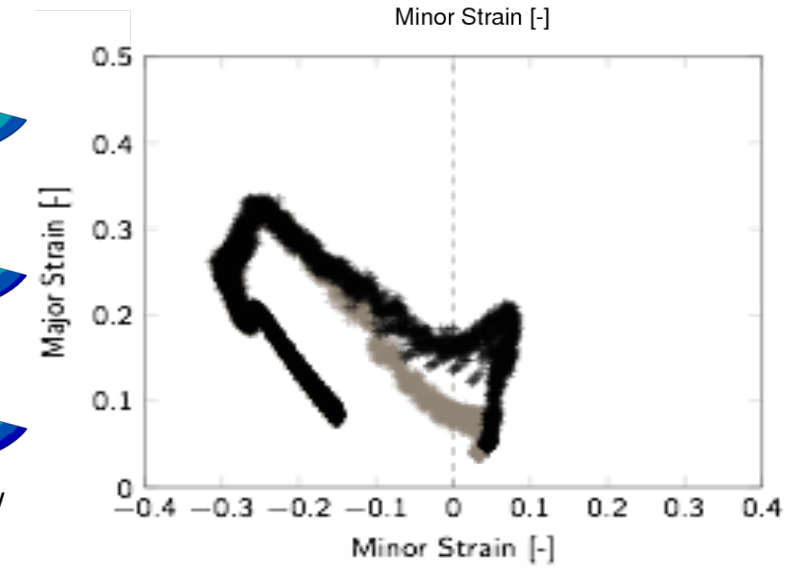
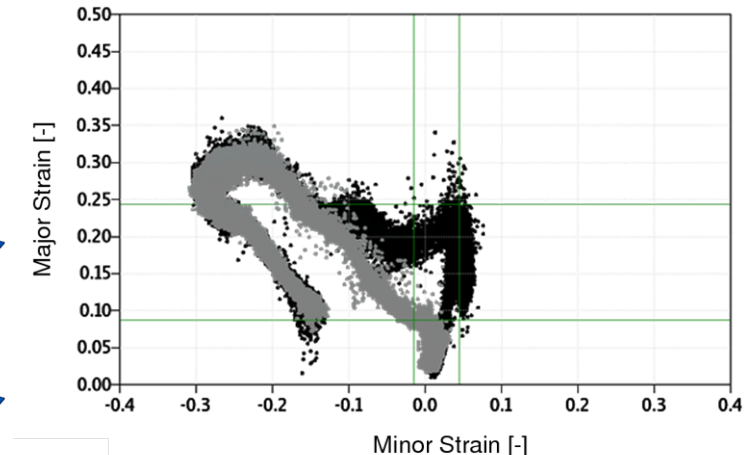
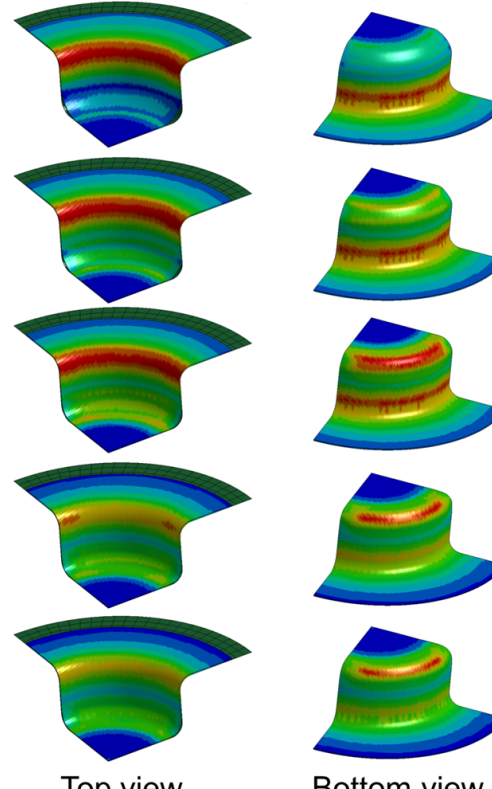
Simulation: Yalin Kiliclar with LS-DYNA

# Combined forming of a round cup

Deep drawing

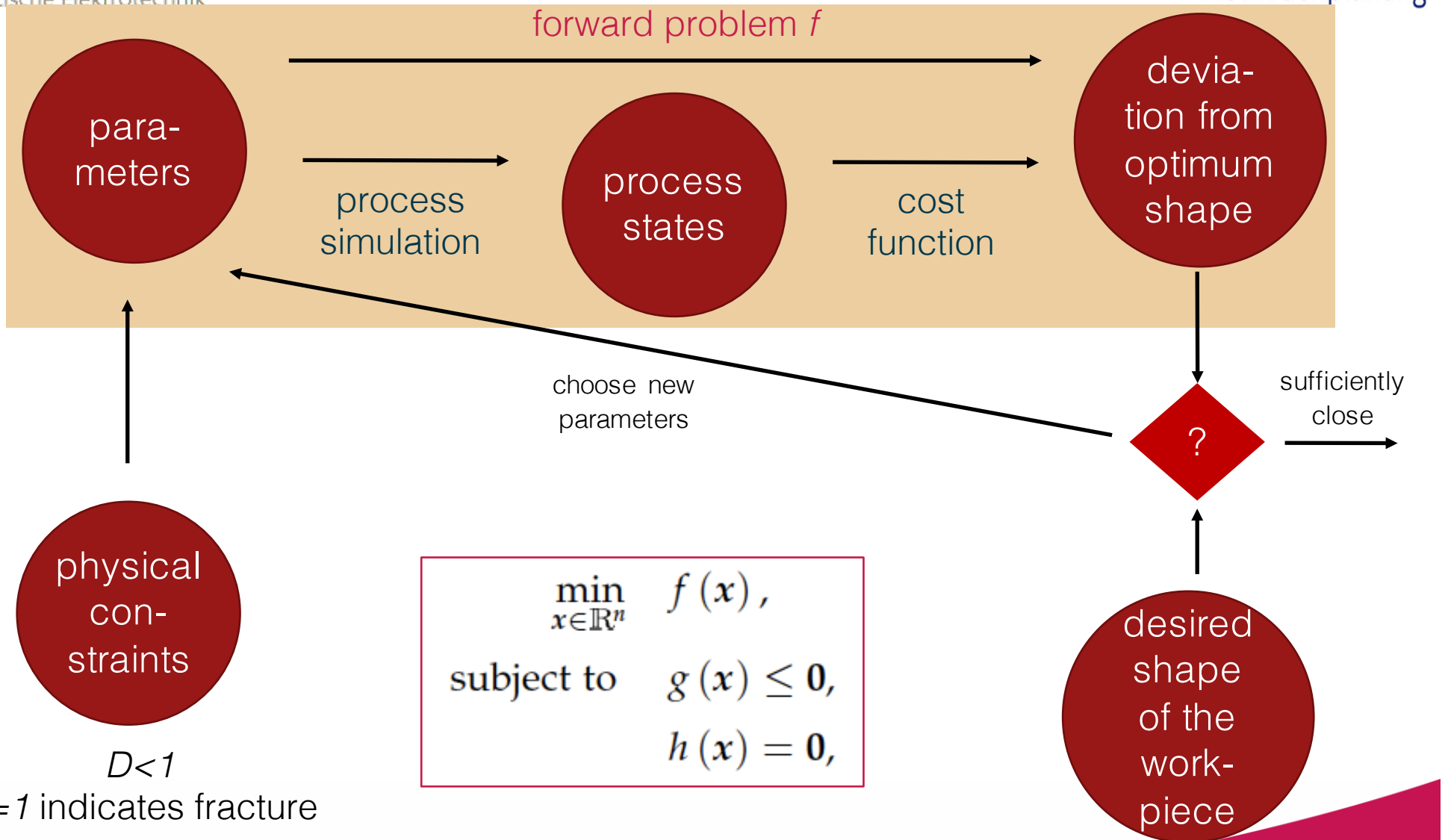


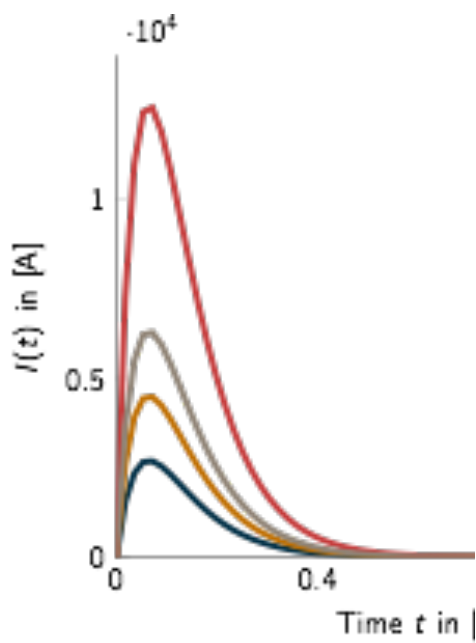
Electromagnetic forming



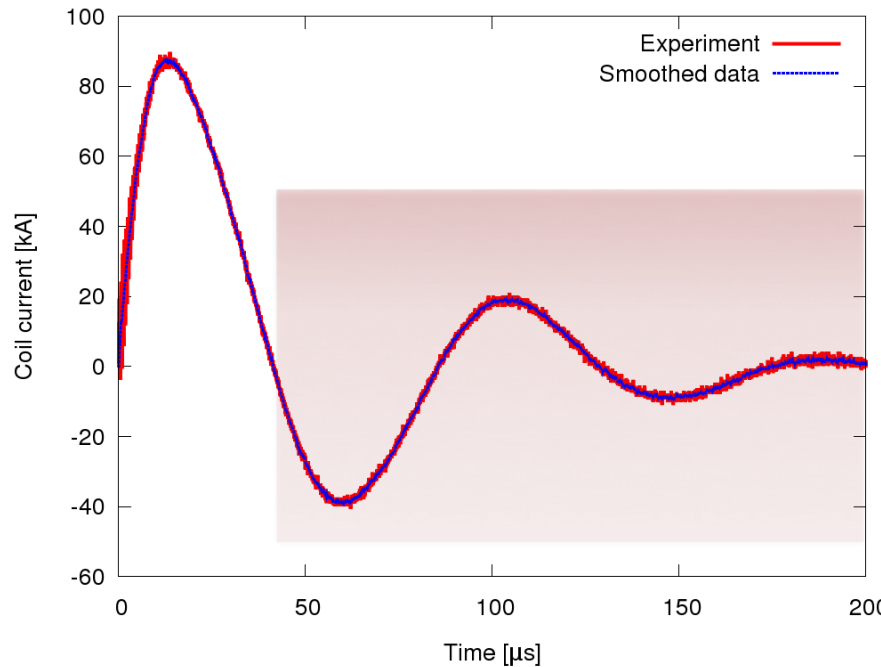
Simulation: Yalin Kiliclar with LS-DYNA

# The inverse problem





# Example: identification of optimum current

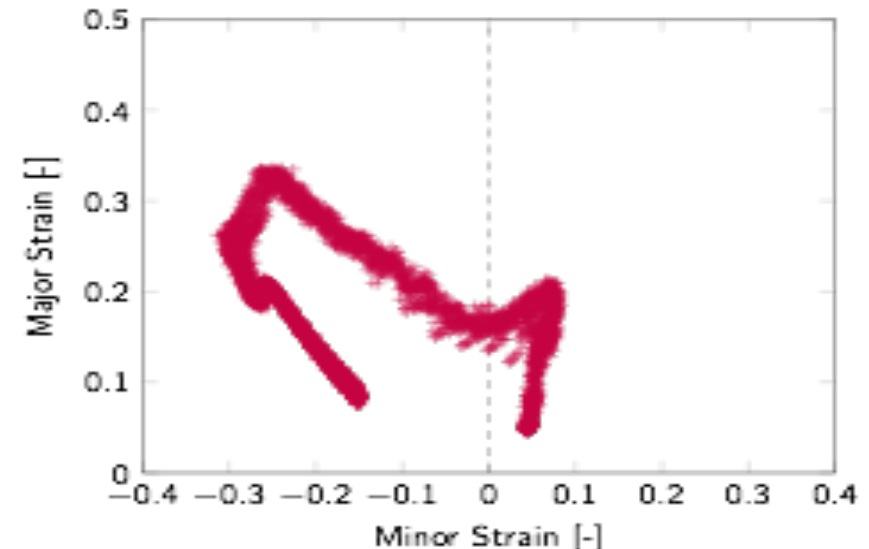


- Only the first half wave is relevant for forming
  - Remaining energy absorbed by coils
  - Try novel approach to reduce wear and energy consumption
- Double exponential pulse as mathematical model

$$I(t) = I_\alpha e^{-\alpha t} + I_\beta e^{-\beta t}$$

# Example: identification of optimum current

- Maximize the radius at bottom edge  
→ Maximize the first principle strain
- Avoid damage  
→ Constrain the damage variable in all elements
- Technically reasonable current  
→ Constrain the current at each time step (here: 125 000 A)

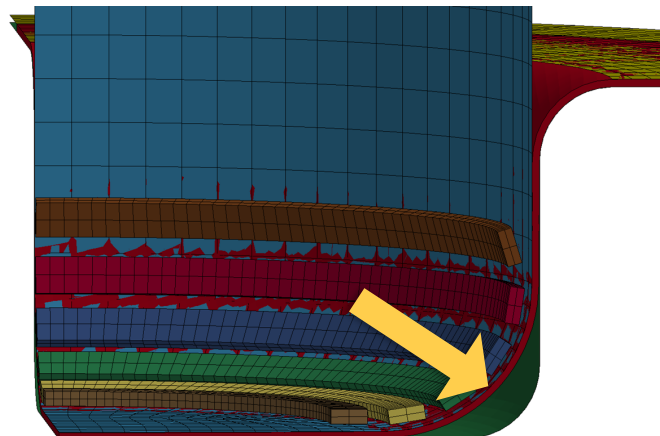


$$\min_{(I_\alpha, I_\beta, \alpha, \beta)^\top \in \mathbb{R}^4} - \sum_{j=1}^m \varepsilon_1^j(I_\alpha, I_\beta, \alpha, \beta),$$

subject to  $D_j(I_\alpha, I_\beta, \alpha, \beta) \leq 1 - p, \quad \forall j = 1, \dots, m,$

$$I_\alpha e^{-\alpha t_i} + I_\beta e^{-\beta t_i} \leq I_{\max}, \quad \forall i = 1, \dots, N.$$

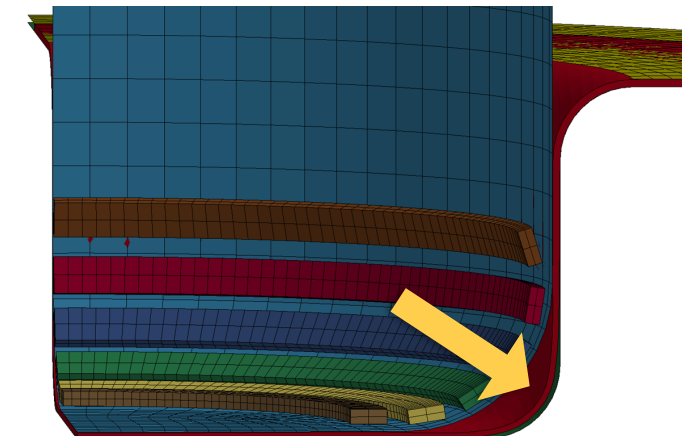
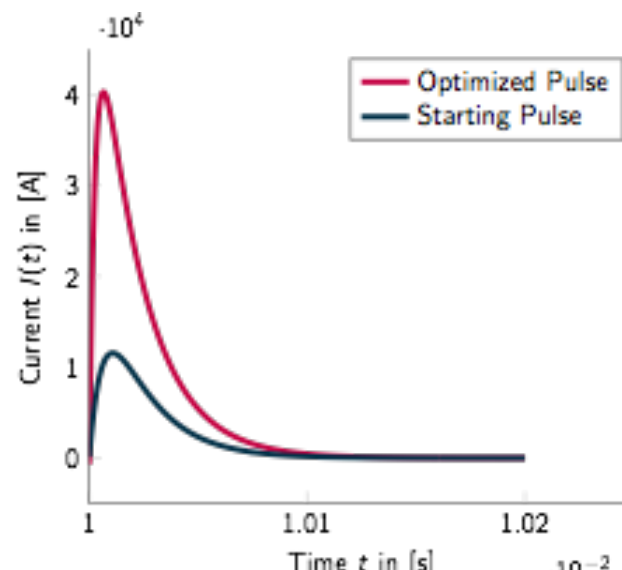
# Example: identification of optimum current



$$r = 20 \text{ mm}$$

$$d = 0.91 \text{ mm}$$

Optimization Method:  
IPOPT as implemented by  
Wächter und Biegler



$$r = 15.35 \text{ mm}$$

$$d = 0.85 \text{ mm}$$

$$I_\alpha = -65570.2 \text{ A}$$

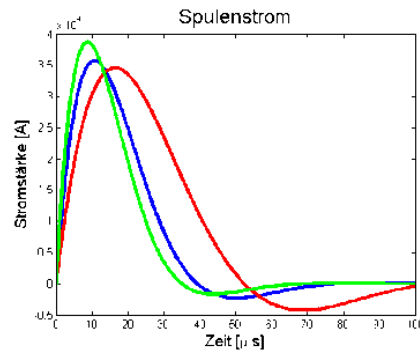
$$I_\beta = 64867.8 \text{ A}$$

$$\alpha = 6878.78$$

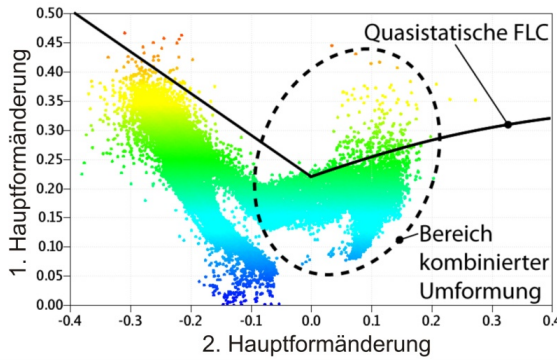
$$\beta = 973.021$$

# Process identification I

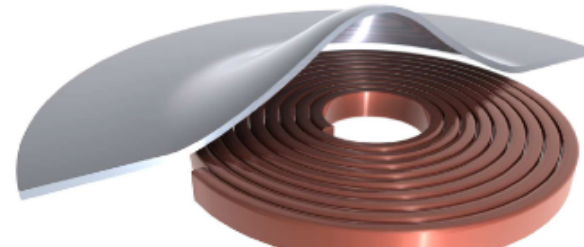
available power



no damage



tool properties

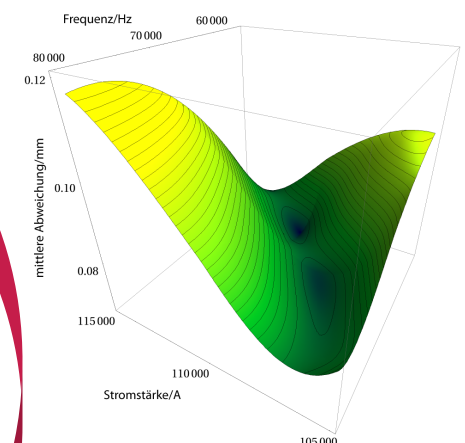


choose process parameters

solve process model  
→ deformation field

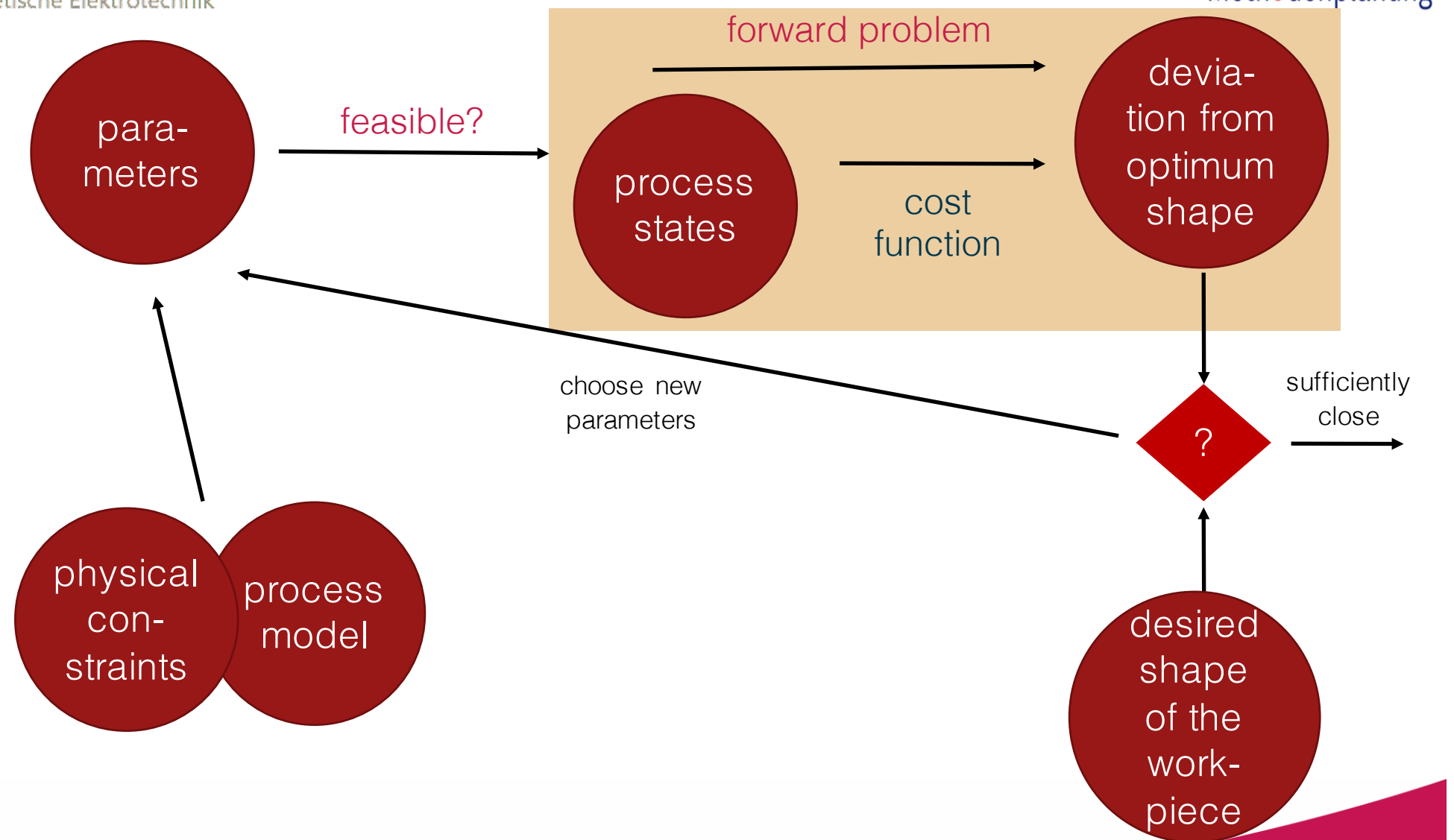
compute deviation  
to optimum shape

economical reasons



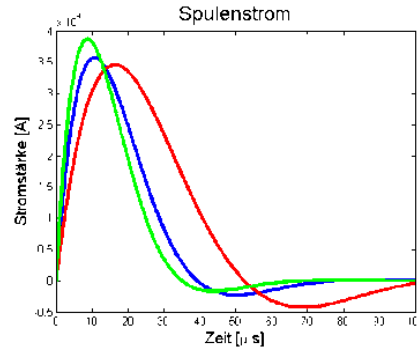
Iterate until  
parameters  
yield a sufficiently  
good result

# The inverse problem II

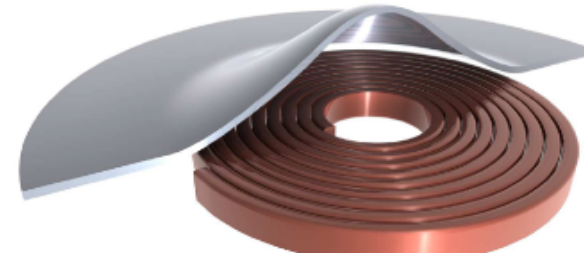


# Process identification II

available power

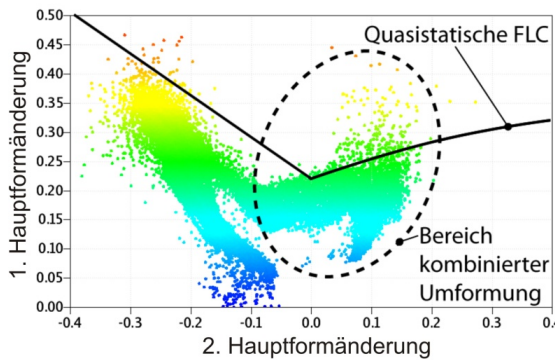


tool properties



conomical reasons

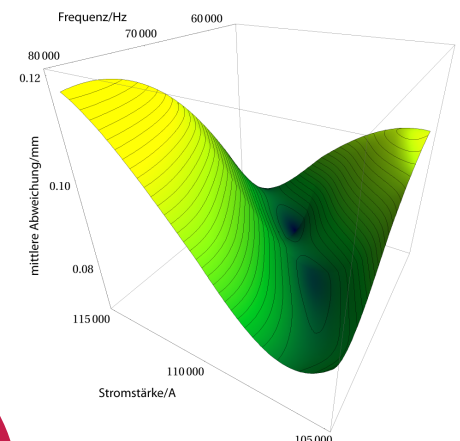
no damage



process model

choose process parameters

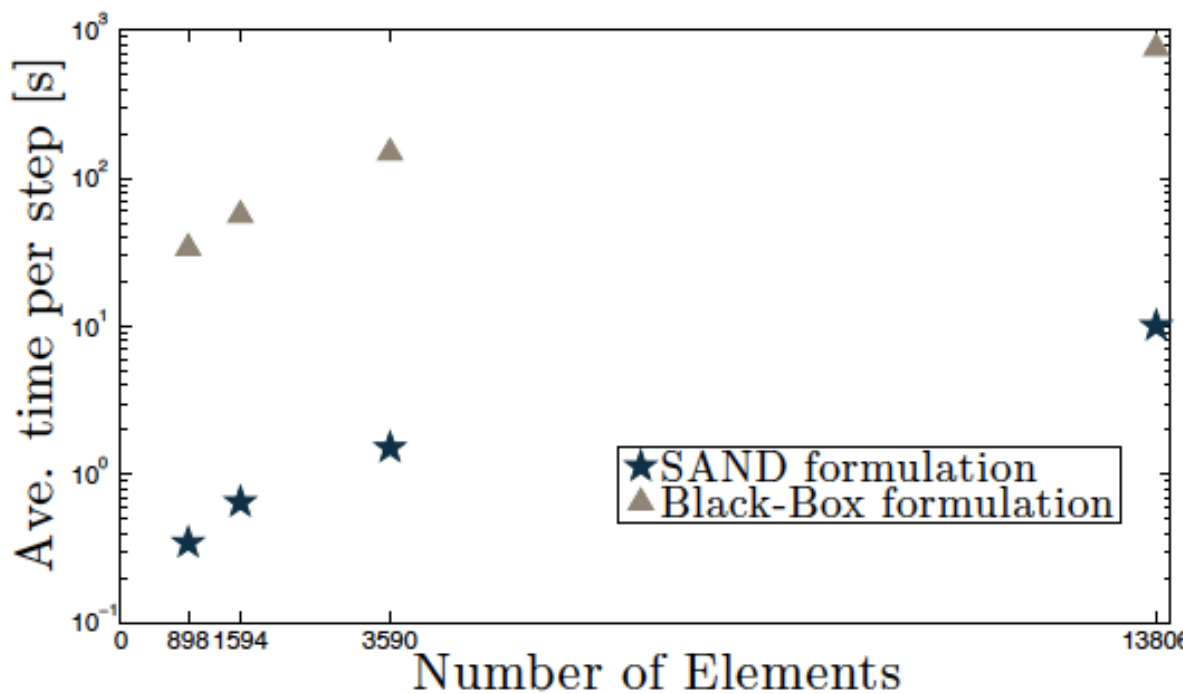
compute deviation to optimum shape



Iterate until parameters yield a sufficiently good result

# Comparison of the methods

- Scheme I allows for a black-box-use of solver and optimizer
- Scheme II requires internal data of the simulation code
- Scheme II is much faster
- Scheme II has not been implemented for the complete problem
- Scheme II produces a huge number of constraints, but simple cost function



Computation time for  
scheme I and II for a  
simple mechanical  
identification problem

Optimization Method: IPOPT as implemented by Wächter und Biegler

# Algorithmic aspects

- Practically, the discrete system of equations with the overall stiffness-matrix of the finite-element model as system matrix is not solved, but given to the optimizing algorithm as constraints
- Also, nonlinearities can be handled by the optimization algorithm
- A large number of constraints can be treated, since only a few of them is active at a certain stage of the algorithmic procedure
- Active set strategies: Only the active constraints need consideration
- Use of simple auxiliary problems in certain areas of the parameter space (trust region methods)

# Shape optimization

Optimization problem

with cost function

such that MQS Maxwell equations hold

Discretized version

$$\Phi(\vec{u}_{\min}) = \min_{\vec{p} \in P, \vec{u}_{\vec{p}} \in V} \Phi(\vec{u}_{\vec{p}}),$$

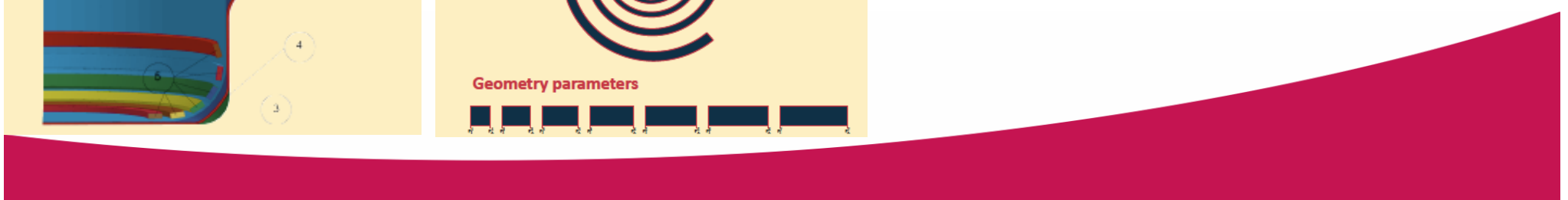
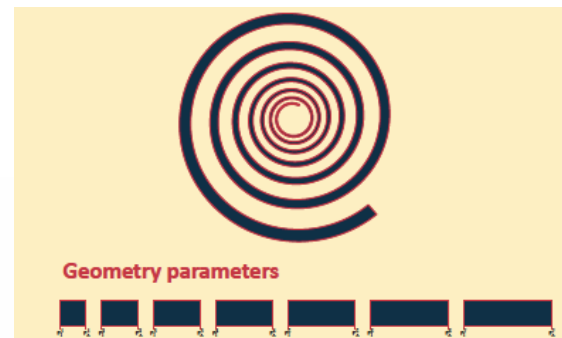
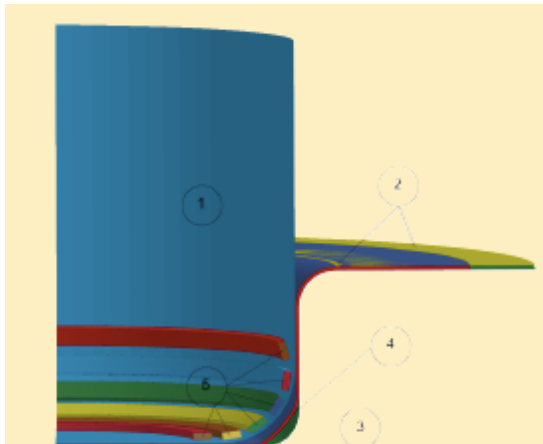
$$\text{s.t. } \Lambda_{\vec{p}} \vec{u}_{\vec{p}} = \vec{f}_{\vec{p}}$$

$$\Phi(\vec{A}_{\vec{p}}) = \int_0^T \int_C \left| \kappa_{\vec{p}} \frac{\partial \vec{A}_{\vec{p}}}{\partial t} \times (\nabla \times \vec{A}_{\vec{p}}) - \vec{f}_{\text{ideal}} \right|^2 dV dt$$

$$\nabla \times \left( \frac{1}{\mu} \nabla \times \vec{A}_{\vec{p}} \right) + \kappa_{\vec{p}} \frac{\partial \vec{A}_{\vec{p}}}{\partial t} = -\kappa_{\vec{p}} \nabla \varphi_{\vec{p}} \\ \text{div } \vec{A} = 0$$

$$\vec{f}_{\text{comp}}(\vec{r}) = \sum_{k \in M} a_k^{(n)} \vec{b}_k(\vec{r})$$

$$\Phi(\vec{q}) = \sum_{n=1}^N \sum_{\vec{q} \in Q} w_n w_{\vec{q}} \left| \vec{f}_{\text{comp}}(\vec{q}) - \vec{f}_{\text{ideal}}(\vec{q}) \right|^2$$



# Summary

- The benefits of high speed forming as part of a process chain can be increased by simulation based method planning
- Virtual planning of complicated processes can efficiently be performed by a full integration of the simulated model into the optimization framework via restrictions – however, then the simulation tool cannot be used as a black-box solver anymore
- Optimization algorithms that can cope with a high number of constraints are available
- Material optimization can be treated with the same algorithm
- Vision: standardized computer software for design problems (inverse problems)